Total Neutron Scattering in Vitreous Silica*

R. J. Breen,† R. M. Delaney, P. J. Persiani, and A. H. Weber
Physics Department, Saint Louis University, St. Louis, Missouri and Argonne National Laboratory, Lemont, Illinois
(Received October 25, 1955; revised version received April 6, 1956)

The structure of Corning superpure vitreous silica glass has been investigated with neutrons. A new method of analysis using variable neutron wavelengths and the measurement of total scattering cross sections from transmission experiments is developed and the results are compared with those from differential x-ray scattering. The total neutron scattering method permits a simple and direct structure analysis with resolution apparently superior to x-rays. The preliminary results compare well in a first approximation analysis with the basic structure model of Warren and others and in addition the neutron-determined atomic radial distribution curve exhibits some finer details than the x-ray results. Thermal inelastic scattering of neutrons was corrected for in an approximate way.

I. INTRODUCTION

THE investigation of structure of liquids by x-ray diffraction has been reviewed by Gingrich.[1] He develops the Zernike-Prins method for differential scattering by liquid elements which leads to the distribution function determining the number of atoms between r and $r+dr$ from any arbitrary (origin) atom within the sample.

With large neutron flux densities available in reactors structure studies using neutron diffraction as a tool have become practicable. Chamberlain[2] investigated the structures of liquid sulfur, lead, and bismuth by measuring the *differential* scattering cross section as a function of $(\sin\theta)/\lambda$. In his work, an essentially constant neutron wavelength was obtained with a crystal spectrometer while the scattering angle was varied to achieve good resolution in $(\sin\theta)/\lambda$.

In the present work the Chamberlain neutron spectrometer[2] originally was used at the Argonne National Laboratory for measuring the differential scattering in vitreous silica. The preliminary, exploratory experiments indicated some desirable features of neutron scattering for glass structure analysis. Because of the complicated corrections and difficulty of normalization of experimental scattering curves inherent in the differential scattering measurements, an alternative method of structure analysis suitable for glasses was developed employing the slow-neutron velocity selector (chopper).[3] The neutron wavelength rather than the scattering angle is varied and the structure analysis is made from the *total* scattering cross section which in turn is obtained from the total (capture plus scattering) cross section directly measured by the transmission method. The results are compared with the x-ray diffraction work of Warren.[4]

* Investigation assisted by the Owens-Illinois Glass Company of Toledo, Ohio, and the U. S. Office of Ordnance Research.
† Now at Westinghouse Electric and Manufacturing Company, Pittsburgh, Pennsylvania.
[1] N. S. Gingrich, Revs. Modern Phys. **15**, 90 (1943).
[2] O. Chamberlain, Phys. Rev. **77**, 305 (1950).
[3] T. Brill and H. Lichtenberger, Phys. Rev. **72**, 585 (1947).
[4] B. E. Warren, J. Am. Ceram. Soc. **17**, 249 (1934); J. Appl. Phys. **8**, 645 (1937).

II. THEORY[5]

The total neutron scattering analysis may be developed by first expressing the theory for structure analysis by x-rays in terms of differential neutron scattering. The radial density distribution for x-ray scattering is[1]

$$4\pi r^2[\rho(r)-\rho_0]=(2r/\pi)\int_0^\infty si(s)\sin rs ds; \quad (1)$$

where $\rho(r)$ is the atomic density as a function of r, ρ_0 is the average atomic density of the sample, $s=4\pi(\sin\theta)/\lambda=4\pi\chi$, θ is half the scattering angle, and $i(s)=(I_{eu}/Nf^2)-1$ where I_{eu} is the differential intensity of scattering in electron units (the ratio of scattered intensity to the intensity scattered by a single electron), N is the number of scattering centers in the sample, and f is the atomic structure factor.

For neutrons $N(d\sigma_s/d\omega)$ replaces I_{eu} and a (nuclear scattering length) replaces f; also[6,7] $4\pi a^2=\sigma_s{}^b$, where $\sigma_s{}^b$ is the coherent scattering cross section for an isolated, bound scattering center. Hence, for differential scattering of neutrons,

$$i(s)=[(4\pi/\sigma_s{}^b)d\sigma_s/d\omega]-1, \quad (2)$$

so that Eq. (1) becomes

$$4\pi r^2[\rho(r)-\rho_0]=(2r/\pi)\times\int_0^\infty s[(4\pi/\sigma_s{}^b)(d\sigma_s/d\omega)-1]\sin rs ds; \quad (3)$$

where the Debye-Waller factor has been neglected as in Eq. (1).

The Fourier transform of Eq. (3) is

$$si(s)=\int_0^\infty 4\pi r[\rho(r)-\rho_0]\sin sr dr. \quad (3a)$$

Integrating the differential scattering cross section over the total solid angle and using $d\omega=2\pi\sin 2\theta d(2\theta)$

[5] The analytical development in this section was suggested by M. Hamermesh.
[6] A. H. Weber, Nucleonics **7**, 31 (1950).
[7] C. G. Shull and E. O. Wollan, Phys. Rev. **81**, 527 (1951).

yields

$$\sigma_s=\int_0^{4\pi} d\omega(d\sigma_s/d\omega),$$

$$=\int_{2\theta=0}^{2\theta=\pi} 2\pi\sin 2\theta d(2\theta)d\sigma_s/d\omega,$$

$$=8\pi\lambda^2\int_0^{1/\lambda}(d\sigma_s/d\omega)\chi d\chi, \quad (4)$$

where $\chi=(\sin\theta)/\lambda$.

Transmission experiments were conducted with the slow neutron velocity selector[3] to measure σ_T, the total cross section for neutrons. The intensity ($\propto$ flux) I of a neutron beam measured after it passes through a sample ($4\frac{1}{2}\times1\frac{1}{2}\times1\frac{1}{4}$ in. with the $1\frac{1}{4}$-in. dimension parallel to the neutron beam) of N_s scattering units per cm^2 is related to the initial beam intensity I_0 by

$$I=I_0\exp[-N_s\sigma_T], \quad (5)$$

whence

$$\sigma_T=N_s\ln(1/T), \quad (6)$$

where the transmission T is the ratio of I to I_0.

The determination of atomic radial density distribution using transmission data requires the integration of the differential scattering cross section by way of Eq. (4), yielding the total scattering cross section which is then experimentally evaluated by using Eq. (6). Substituting Eq. (2) in Eq. (4) and using $s=4\pi\chi$ yields (writing σ_{Ls}, the total liquid sample scattering cross section, for σ_s)

$$\sigma_{Ls}=\frac{\sigma_s{}^b\lambda^2}{8\pi^2}\left(\int_0^{4\pi/\lambda} sds+\int_0^{4\pi/\lambda} si(s)ds\right). \quad (7)$$

Integrating the first term and using Eq. (3a) in the second term of the right-hand side of Eq. (7) yields

$$\frac{\sigma_{Ls}}{\sigma_s{}^b}=1+\frac{\lambda^2}{8\pi^2}\int_0^{4\pi/\lambda}\int_0^{\infty} 4\pi[\rho(r)-\rho_0]\sin srdrds. \quad (8)$$

Integration with respect to s yields

$$\frac{\sigma_{Ls}}{\sigma_s{}^b}=1+\frac{\lambda^2}{2\pi}\int_0^{\infty}[\rho(r)-\rho_0][1-\cos(4\pi r/\lambda)]dr. \quad (9)$$

Taking[8]

$$\int_0^{\infty}[\rho(r)-\rho_0]dr=0, \quad (10)$$

setting $\alpha=4\pi/\lambda$ and $i(\alpha)=1-\sigma_{Ls}/\sigma_s{}^b$, and rearranging, yields

$$\left(\frac{\alpha^2}{4\pi}\right)i(\alpha)=\frac{2}{\pi}\int_0^{\infty}[\rho(r)-\rho_0]\cos\alpha r dr. \quad (11)$$

[8] If by definition $\bar{\rho}=\lim_{R\to\infty}(\int_0^R\rho(r)dr/\int_0^R dr)$, it can be shown that $\bar{\rho}=\rho_0$ to a close approximation for R large compared to interatomic distances.

Multiplying both sides of Eq. (11) by $\cos\alpha r'$ and integrating with respect to α over the range 0 to ∞ yields

$$\frac{1}{4\pi^2}\int_0^{\infty}\alpha^2 i(\alpha)\cos\alpha r'd\alpha=\frac{2}{\pi}\int_0^{\infty}\cos\alpha r'd\alpha \times\int_0^{\infty}[\rho(r)-\rho_0]\cos\alpha r dr. \quad (12)$$

Since the right-hand side of Eq. (12) is the Fourier integral representation of $[\rho(r)-\rho_0]$, the radial density distribution is given by the corresponding transform

$$4\pi r^2[\rho(r)-\rho_0]=\frac{r^2}{\pi}\int_0^{\infty}\alpha^2 i(\alpha)\cos\alpha r d\alpha. \quad (13)$$

If the analysis is extended to a diatomic substance such as vitreous silica, four radial densities, instead of the single $\rho(r)$ of (13), must be considered: $\rho^{ii}(r)$, the radial density of i-type atoms about an i-type origin atom; $\rho^{jj}(r)$, of j-type atoms about a j-type atom; $\rho^{ij}(r)$, of j-type atoms about an i-type atom; and $\rho^{ji}(r)$, of i-type atoms about a j-type atom. In the present work it is assumed that of the four distributions involved in the radial densities, the first two and the third and fourth together are independent of one another; that is, they do not overlap. This assumption is substantiated by the ultimate experimental results.

Hence, for vitreous silica, Eq. (13) (for a monatomic substance) is replaced by the following three expressions.

(1) For the $i-i$ system (i-type atoms about an i-type atom)

$$4\pi r^2 f_i\{\rho^{ii}(r)-\rho_i\}=\frac{r^2}{\pi}\int_0^{\infty}\alpha^2 i_1(\alpha)\cos\alpha r d\alpha; \quad (14)$$

(2) for the $j-j$ system (j-type atoms about a j-type atom)

$$4\pi r^2 g f_j\{\rho^{jj}(r)-\rho_j\}=\frac{r^2}{\pi}\int_0^{\infty}\alpha^2 i_1(\alpha)\cos\alpha r d\alpha; \quad (15)$$

(3) for the $i-j$ and $j-i$ systems

$$4\pi r^2 g^{\frac{1}{2}}[f_j\{\rho^{ji}(r)-\rho_i\}+f_i\{\rho^{ij}(r)-\rho_j\}]=\frac{r^2}{\pi}\int_0^{\infty}\alpha^2 i_1(\alpha)\cos\alpha r d\alpha. \quad (16)$$

In Eqs. (14) to (16)

$$i_1(\alpha)=[\sigma_{sc}-(\sigma_{obs}-\sigma_a)]/\sigma_i, \quad (17)$$

where σ_{sc} is the bound isolated scattering cross section for the molecule, σ_{obs} is the total experimentally measured (chopper) cross section, σ_a is the capture cross section for the molecule [thus $\sigma_{obs}-\sigma_a$ replaces σ_{Ls} of Eqs. (7) to (13)] and σ_i is the bound coherent scattering cross section for the i-type atom. Also, f_i and f_j are the fractions of i- and j-type atoms in the diatomic sub-

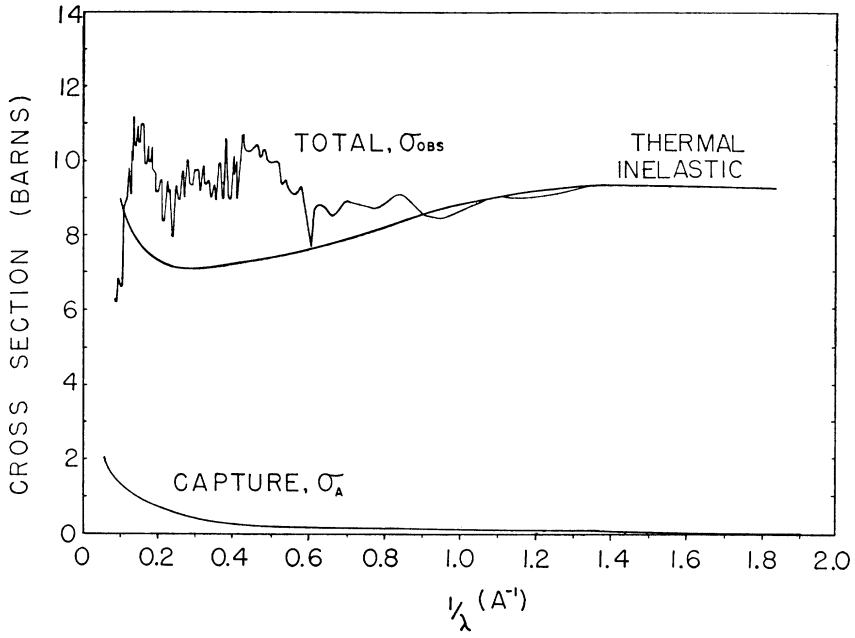

FIG. 1. Neutron cross sections for superpure Corning vitreous silica. The observed total (capture plus scattering) cross section σ_{obs} curve is plotted directly from data obtained with the chopper. Counting statistics: probable error 5% or smaller. Resolution; $\Delta(1/\lambda)$ at half-maximum is $0.012\ A^{-1}$ at $1/\lambda = 0.625\ A^{-1}$.

stance; g is σ_j/σ_i; ρ_i and ρ_j are the average radial densities of the i-type atoms in the $i-i$ system and the j-type atoms in the $j-j$ systems, respectively, and are defined by

$$\rho_i = \int_0^R 4\pi r^2 \rho^{ii}(r)dr \Big/ \int_0^R 4\pi r^2 dr, \qquad (18)$$

$$\rho_j = \int_0^R 4\pi r^2 \rho^{jj}(r)dr \Big/ \int_0^R 4\pi r^2 dr. \qquad (19)$$

It is emphasized that Eqs. (14) to (16) constitute a "separate-systems" analysis and may be used only when the separate radial densities present act independently. This means, for example, that the $i-i$ system alone produces a peak at distance r in the radial density distribution curve, the effect of the $j-j$, $i-j$, and $j-i$ in phase scattering being negligible at the same distance r; and so on. If such is not the case, Eqs. (14) to (16) must be modified which can be done.

III. ANALYTICAL PROCEDURE

The measurement of the total cross section of Eq. (6) with the chopper is straightforward. The transmission coefficient is calculated by the ratio of the cadmium difference reading with the sample in the beam to the cadmium difference reading without the sample. Figure 1 shows the total cross section σ_{obs} so obtained for superpure Corning vitreous silica. This observed total cross section includes the coherent liquid scattering (the interferent part), capture (designated by σ_a), incoherent elastic scattering (spin and isotope effects), thermal incoherent scattering (decreased coherent scattering calculated by the Debye-Waller factor), and thermal inelastic scattering.

The capture cross section is readily subtracted [as indicated by Eq. (17)] from the total cross section on a σ *vs* λ plot since σ_a is linear with λ.[9] Since the capture cross section is zero for $\lambda = 0$, one other point[10] was used to determine the σ_a *vs* λ straight line.

The incoherent elastic part of the scattering is zero, since for vitreous silica the nuclei involved are monoisotopic and of spin zero. The thermal decreased coherency is small for vitreous silica and so was neglected. The thermal inelastic scattering cross section was evaluated approximately by assuming it to be proportional to the reciprocal Debye temperature and using the curves given by Cassels.[11] The resulting curve was fitted to the experimental curve in the region $1.1\ A^{-1} < 1/\lambda < 2\ A^{-1}$ as is indicated by Fig. 1 and was used as σ_{se} in Eq. (17). This means that $\sigma_{obs} - \sigma_a$ approaches the thermal inelastic cross section at the shorter neutron wavelengths here employed. Also, the resulting correction is a one-phonon correction at large wavelength and a Debye-Waller type correction at small wavelength and is an approximation. Incidentally, the value of σ_{Ls} at the maximum value of $1/\lambda$ in Fig. 1 is σ_s^b of Eqs. (7) to (13).

The integrals of Eqs. (14) to (17) were evaluated by representing them as finite sums[12]; a 128-point analysis (using an electronic digital computer) was

[9] P. J. Bendt and I. W. Ruderman, Phys. Rev. **77**, 575 (1950).
[10] *Nuclear Data*, National Bureau of Standards Circular No. 499 (U. S. Government Printing Office, Washington, D. C., 1950).
[11] O. R. Frisch, *Progress in Nuclear Physics* (Academic Press, Inc., New York, 1950), Vol. 1, p. 206.
[12] G. C. Danielson and C. Lanczos, J. Franklin Inst. **223**, 365 (1942); **233**, 435 (1942).

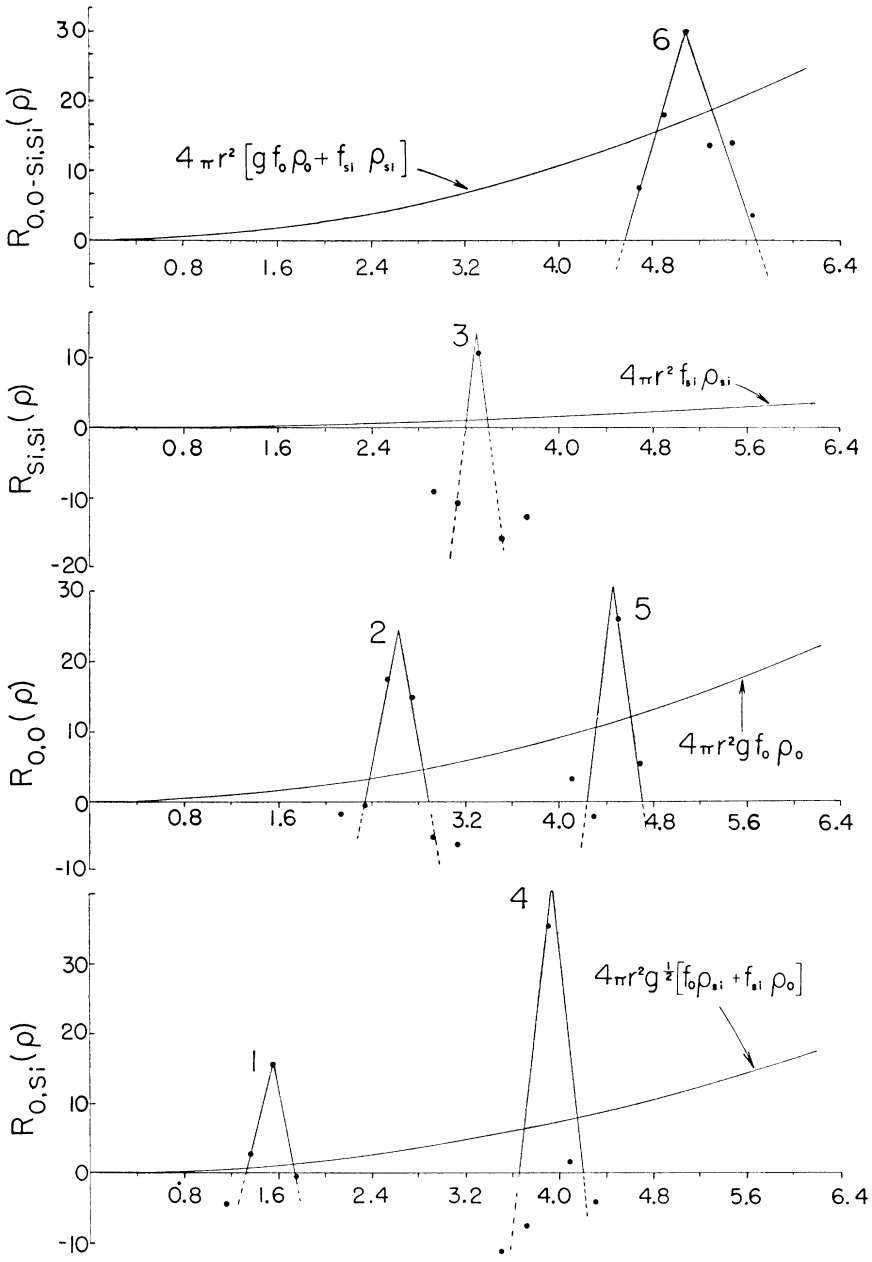

FIG. 2. Atomic radial density distribution for superpure Corning vitreous silica obtained by a 128-point analysis of the data of Fig. 1. The peaks are numbered 1–6 in order of increasing radial distance r: peak 1 is for O atoms about a Si origin atom or for Si atoms about an O origin atom; peak 2 is for O atoms about an O origin atom; peak 3 is for Si atoms about a Si origin atom; peak 4 is for 2nd Si atoms about an O origin atom or for 2nd O atoms about a Si origin atom; peak 5 is for 2nd O atoms about an O origin atom; peak 6 is for 2nd Si atoms about a Si origin atom and 3rd O atoms about an O origin atom.

employed to obtain the radial density distribution curves of Fig. 2.[13]

[13] The ordinates in Fig. 2 are defined as follows:

$$R_{O,O-Si,Si}(\rho) \equiv 4\pi r^2[g f_O \rho^{O,O} + f_{Si}\rho^{Si,Si}] = 4\pi r^2[g f_O \rho_O + f_{Si}\rho_{Si}] + \frac{r^2}{\pi}\int_0^\infty i_1(\alpha)\alpha^2 \cos\alpha r d\alpha;$$

$$R_{Si,Si}(\rho) \equiv 4\pi r^2 f_{Si}\rho^{Si,Si} = 4\pi r^2 f_{Si}\rho_{Si} + \frac{r^2}{\pi}\int_0^\infty i_1(\alpha)\alpha^2 \cos\alpha r d\alpha;$$

$$R_{O,O}(\rho) \equiv 4\pi r^2 g f_O \rho^{O,O} = 4\pi r^2 g f_O \rho_O + \frac{r^2}{\pi}\int_0^\infty i_1(\alpha)\alpha^2 \cos\alpha r d\alpha;$$

$$R_{O,Si}(\rho) \equiv 4\pi r^2 g^{\frac{1}{2}}[f_O \rho^{O,Si} + f_{Si}\rho^{Si,O}] = 4\pi r^2 g^{\frac{1}{2}}[f_O \rho_{Si} + f_{Si}\rho_O] + \frac{r^2}{\pi}\int_0^\infty i_1(\alpha)\alpha^2 \cos\alpha r d\alpha.$$

IV. RESULTS AND DISCUSSION

The areas under the peaks of the radial density distribution curves (Fig. 2) yield the number of atoms (O or Si) located about an origin atom (O or Si) at the average distance given by the r value of the peak. In calculating these numbers of atoms the basic unit structure of Warren[4] was used as a working model. In this structure each Si atom is tetrahedrally surrounded by four O atoms; the vertices of the first tetrahedron are at the same time vertices of four other tetrahedra so that each O atom is bound to two Si atoms. (In the glassy state this structure is not repeated at regular

intervals; there are distortions so that some features of a random network are produced.)

Thus if the first definite peak of Fig. 2 (at $r=1.6$ A approximately, labeled 1) is considered to be produced by the smallest Si—O distances, then from Eq. (16)

$$G(r)=4\pi r^2 g^{\frac{1}{2}}\{f_O\rho^{O-Si}(r)+f_{Si}\rho^{Si-O}(r)\}$$
$$=4\pi r^2 g^{\frac{1}{2}}\{f_O\rho_{Si}+f_{Si}\rho_O\}$$
$$+\frac{r^2}{\pi}\int_0^\infty \alpha^2 i_1(\alpha)\cos\alpha r d\alpha, \quad (20)$$

and

$$\int_{r_1}^{r_2} G(r)dr=\text{area under Si—O peak}$$
$$=g^{\frac{1}{2}}\{f_O N^{O-Si}+f_{Si}N^{Si-O}\}, \quad (21)$$

where $N^{O-Si}=2$ is the number of Si atoms about an O atom near $r=1.6$ A. Using the triangle approximation method for measuring the area under the peak yields N^{Si-O}, the number of O atoms about a Si atom at a distance near 1.6 A. The bound-isolated scattering cross-section values used were 2.25 barns (silicon) and 3.6 barns (oxygen).[14]

This procedure was followed for the first 6 peaks as shown by Fig. 2, and the results of the analysis are listed in Table I. The experimental total neutron scattering values for the number of atoms at the various distances are approximate only since the triangle form of the peaks is determined by a few points only.

Satisfactory agreement of the experimental values, both of interatomic distances and numbers of atoms located at these approximate distances, with corresponding values calculated from the Warren model is found. Actually, the total neutron scattering results are better and more informative than are Warren's x-ray determinations[4] in several ways, as follows: (1) The neutron scattering yields better resolution than the x-rays for the O—O (2.65 A) and Si—Si (3.20 A) distances; these peaks are smeared into a single broad peak for x-rays. (2) A peak appears clearly at the O—2nd O distance (4.50 A) for neutrons; a minimum actually is found with x-rays. (3) The Si—2nd O distance (4.00 A) is found somewhat more precisely with neutrons (3.9 A) than with x-rays (4.2 A). (4) The

[14] *Neutron Cross Sections*, Atomic Energy Commission Report AECU-2040 (Technical Information Division, Department of Commerce, Washington, D. C., 1952).

TABLE I. Atomic radial density distribution results for Corning superpure vitreous silica (Fig. 2) compared with Warren's model.[a]

Proposed interatomic distance (first-noted atom is origin atom)	Warren model		Total neutron scattering	
	Distance (A)	No. of atoms	Distance (A)	No. of atoms (exptl. values, from areas under peaks of Fig. 2)
Si—O	1.60	4 O	1.6	4.3
O—O	2.65	6 O	2.6	6.6
Si—Si	3.20	4 Si	3.3	2.7
Si—2nd O	4.00	12 O	3.9	13.8
O—2nd O	4.50	6 O / 18 O [b]	4.5	6.9
Si—2nd Si	5.20	12 Si	5.1	12.0

[a] See reference 4.
[b] A 3-dimensional model of SiO_2 tetrahedral units yields a total of 18 O atoms at the Si—2nd O spacing if a rigid radial orientation is followed; deviations from strict radial orientation, permitting a more compact filling of space, probably causes one O atom of each 3 basal O atoms to be nearer to the origin atom, yielding 6 as the number of O atoms at the O—2nd O distance.

neutron scattering indicates that the number of second oxygens about an oxygen atom is six, suggesting that outlying SiO_2 tetrahedra (the four tetrahedra which are joined at their vertices to a central "origin" tetrahedron) are oriented in such a way as to bring one O atom of each three O atoms in the triangular base plane of the SiO_2 tetrahedra somewhat closer to an O origin atom than the remaining two O atoms.

Thus the total neutron scattering results confirm, as a first approximation, Warren's vitreous silica structure model. As noted, neutron diffraction appears superior in resolution to x-rays and permits some refinements in the Warren model and in addition much larger values of $1/\lambda$ can be achieved, thus permitting accurate evaluation of data in the region beyond interference effects. It is clear that the thermal inelastic scattering correction is of importance in the neutron work.

V. ACKNOWLEDGMENTS

It is a distinct pleasure to acknowledge the abiding interest and cooperation of O. G. Burch and H. H. Holscher of the Owens-Illinois Glass Company (Toledo) and of J. C. Boyce and L. A. Turner of the Argonne National Laboratory. Many of the regular staff of the Argonne National Laboratory contributed scientifically including especially M. Hamermesh, A. Wattenberg, O. Chamberlain, and R. Ringo; D. Meneghetti gave assistance in collecting the data. More recently the U. S. Office of Ordnance Research has aided materially in continuing this necessarily long-range research.